

Influence of Concrete Material Ductility on Shear Response of Stud Connections

by Shunzhi Qian and Victor C. Li

This paper presents an experimental study on the influence of concrete material ductility on the shear response of stud connections, including failure mode, ultimate strength, slip capacity, and structural integrity. A series of pushout specimens were tested for this evaluation by using a unique strain-hardening fiber-reinforced engineered cementitious composite (ECC). Tension-softening steel fiber-reinforced concrete (SFRC) and normal concrete (both plain and steel bar reinforced) were adopted as the reference materials. The experimental results show that the stud connections with ECC exhibit more ductile failure mode, and a higher ultimate strength and slip capacity compared with connections with other concrete materials, in addition to a much improved structural integrity. The superior ductility of ECC was clearly reflected by microcrack development near the shear studs, suppressing the localized fracture mode typically observed in other concrete materials. This significant enhancement of ductility suggests that the use of an ECC material can be effective in redistributing loads among the shear studs and in improving composite action between steel girders and concrete bridge decks.

Keywords: composites; ductility; failure; shear; strength.

INTRODUCTION

Currently, stud connectors are widely used in beams and bridge girders to form composite action between steel and concrete. Composite beams have gained popularity in bridges since the 1950s due to the contributions of Viest on the stud shear connectors (1956a,b; 1960). Their primary growth in building construction was a result of the simplified design provisions introduced into the 1961 AISC specification (Driscoll and Slutter 1961). The work done at Lehigh University (Ollgaard et al. 1971) and later introduced into AASHTO and AISC specifications provided guidelines for the use of lightweight and normalweight concrete in the composite beams.

Thus far, research on stud connections is conducted at two levels: the pushout subassembly level and composite beam level. Test results from pushout specimens can be used for designing composite beams because they give conservative values of the ultimate strength (Driscoll and Slutter 1961). Previous research (Ollgaard et al. 1971; Oehlers and Foley 1985; Yen et al. 1997; Bursi and Gramola 1999) on both levels revealed that concrete fracture contributed to the failure of pushout specimens or composite beams, as can be seen in Fig. 1. As illustrated by the pushout specimen in Fig. 1(a), the concrete was fractured on one side of the stud shank due to the stress concentration near the stud head. On the other side of the stud shank, the concrete was crushed due to high bearing stress of the shank of the stud. Figure 1(b) shows the failure of a composite beam under flexural loading, where the test configuration is shown in Figure 1(c). Failure occurs by a longitudinal splitting crack between two rows of shear studs.

Until now, the research on stud connections has only concentrated on systems involving steel studs in concrete and mortar. Because the catastrophic fracture failure may be attributed to high stress concentration induced by the stiff steel stud bearing against the brittle concrete materials, it seems that using a more ductile concrete material may result in improved performance for stud connections in terms of structural strength, ductility, and integrity.

A number of recent studies have indicated that engineered cementitious composites (ECC) (Li 1993), a unique type of high-performance fiber-reinforced cementitious composites (HPFRCCs), shows promise in overcoming the stress concentration problems (Li 1998). Based on a micromechanics design approach, ECC shows strain hardening behavior in tension accompanied by saturated multiple cracking, while only using a small volume fraction of fibers (typically less than 2%). Particularly, unlike brittle concrete/mortar, ECC

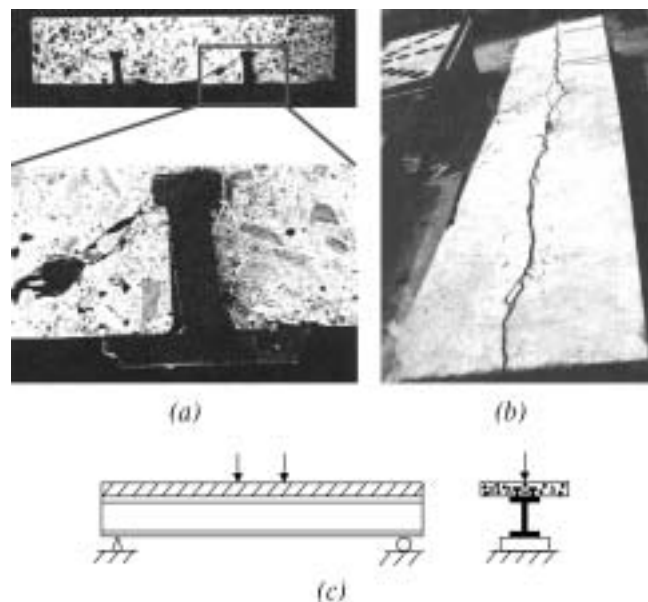


Fig. 1—(a) Sawed sections of pushout specimen showing fracture of concrete (Ollgaard et al. 1971); (b) composite beam failed by longitudinal splitting crack between two rows of shear studs (Yen et al. 1997); and (c) test configuration of stud connection on the composite beam level (Yen et al. 1997).

ACI Materials Journal, V. 103, No. 1, January-February 2006.

MS No. 04-370 received November 12, 2004, and reviewed under Institute publication policies. Copyright © 2006, American Concrete Institute. All rights reserved, including the making of copies unless permission is obtained from the copyright proprietors. Pertinent discussion including authors' closure, if any, will be published in the November-December 2006 *ACI Materials Journal* if the discussion is received by August 1, 2006.

ACI member **Shunzhi Qian** is a PhD candidate in the Department of Civil and Environmental Engineering, the University of Michigan, Ann Arbor, Mich. He received his BSE in civil engineering from Southeast University, Nanjing, and his MS in highway engineering from the Research Institute of Highway, Beijing, China. His research interests include the application of high-performance fiber-reinforced cementitious composites to highway engineering and other infrastructure systems.

ACI member **Victor C. Li** is a professor in the Department of Civil and Environmental Engineering at the University of Michigan. He is a member of ACI Committee 544, Fiber Reinforced Concrete. His research interests include the design of ultra ductile and green cementitious composites, their application to innovative infrastructure systems, and integration of materials and structural design.

reveals a high damage-tolerant behavior under stress concentration induced by steel/concrete interaction in a number of experimental studies (Kanda et al. 1998; Parra-Montesinos and Wight 2000; Li 2002; Kesner and Billington 2002) involving subassemblages where steel and concrete/ECC come into contact with one another. These observations suggest the possibility of adopting ECC to replace concrete in stud connections to avoid fracture failure.

As mentioned previously, the primary cause for brittle fracture failure of concrete in stud connections is its brittleness. With a tensile strain capacity of approximately 3% and fracture energy of 34 kN/m (194 lb/in.) (approximately three orders of magnitude those of normal concrete, which typically has corresponding value of 0.01% and 30 N/m [0.17 lb/in.], respectively) in ECC, the use of this material is expected to switch the failure mode from brittle concrete failure to ductile ECC yielding or even steel stud shank yielding in the stud connection. The corresponding structural ductility (slip capacity) and strength of the ECC/shear connection system may be enhanced because the presence of ECC allows plastic yielding of the matrix material, delaying the onset of final fracture failure if it happens at all. The enhanced ductility of stud connections should aid in redistributing the

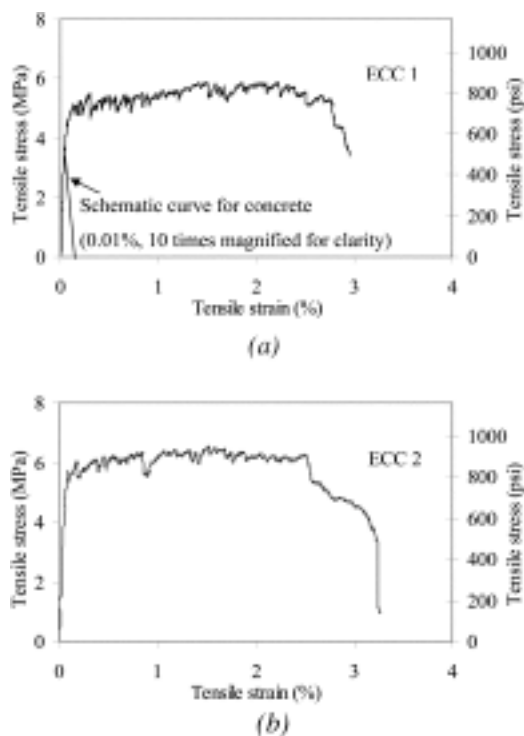


Fig. 2—Uniaxial tensile stress-strain curve of: (a) ECC 1; and (b) ECC 2 tested with plate specimens of 12.7 x 76.2 x 304.8 mm (0.5 x 3 x 12 in.).

load among nearby shear studs, particularly important for a precast bridge deck system where shear connectors are evenly distributed in the shear span while the horizontal shear force is not uniform.

The objective of this study is to investigate the influence of stud ductility of ECC material on the shear response of stud connections on the pushout specimen level, and the feasibility of using ductile ECC to replace concrete in stud connections to enhance the performance of structures with stud connectors.

RESEARCH SIGNIFICANCE

A new approach and material solution—using material ductility to overcome brittle concrete fracture failure in steel/concrete interaction zones—are proposed and investigated preliminarily. In this study, special attention is paid to the use of ECC ductility to avoid concrete catastrophic failure in stud connections of composite structures. In addition to a more desirable failure mode, ECC/stud connections can achieve significantly higher structural strength, ductility, and integrity, which is demonstrated by pushout test results with different concrete materials, including ECC, SFRC, reinforced concrete (RC), and plain concrete. This significant enhancement of structural response suggests that the use of ECC materials can be effective in redistributing loads among the shear studs and in improving composite action between steel girders and concrete bridge decks.

EXPERIMENTAL PROGRAM

Materials

The investigated concrete materials with significantly different tensile strain capacity (material ductility) are shown in Test Group 1 of Table 1, including Concrete 1, RC 1, SFRC 1, and ECC 1. The ECCs adopted in the present study have a tensile strain capacity approximately 250 times that of normal concrete. Group 2 (Concrete 2 and ECC 2) was used to investigate the influence of compressive strength on the shear response of the stud connections. Groups 1 and 2 have target compressive strengths of 55 and 40 MPa (8.0 and 5.8 ksi), respectively. The actual compressive strength realized is listed in Table 2.

By uniaxial tension test, both ECC 1 and 2 show a strain capacity around 2.5% at 28 days, revealed in Fig. 2. The

Table 1—Mixture proportions of different concrete materials by weight (fiber by volume)

Material	Target f'_c , MPa (ksi)	ϵ_u , %	C	S	CA	FA	W	HRWRA	Fiber
Concrete 1	55 (8.0)	0.01*	1	1.3	1.3	0	0.36	0.01	0
RC 1	55 (8.0)	0.01*	1	1.3	1.3	0	0.36	0.01	0
SFRC 1	55 (8.0)	0.1*	1	1.3	1.3	0	0.36	0.01	Steel (0.01)
ECC 1	55 (8.0)	2.5	1	0.8	0	1.2	0.53	0.03	PVA (0.02)
Concrete 2	40 (5.8)	0.01*	1	2	2	0	0.45	0.01	0
ECC 2	40 (5.8)	2.5	1	0.8	0	1.2	0.58	0.03	PVA (0.02)

*Assumed value.

Notes: Target f'_c = target compressive strength; ϵ_u = uniaxial tensile strain capacity; C = Type 1 portland cement; S = silica sand F110 for ECC 1 and ECC 2, ASTM C 778 sand for Concrete 1, 2, RC 1, and SFRC 1; CA = coarse aggregate with maximum size for 19 mm (3/4 in.); FA = Type F fly ash; W = water; HRWRA = high-range water-reducing admixture; PVA fiber = polyvinyl alcohol fiber; steel fiber = hooked-end steel fiber. Reinforcement ratios in RC specimens are 0.56 and 0.86% in longitudinal and transverse direction, respectively (totally four layers), similar to that used in Ollgaard et al. (1971).

modulus of elasticity of concrete and ECC were measured by using standard cylinder specimens in compression test. It is worth mentioning that the modulus measured from both compression test and uniaxial tension test of ECC specimens agree well.

The shear studs used in this test were made from Grade 1018 cold-drawn bars, conforming to AASHTO M169 (ASTM A 108), “Standard Specification for Steel Bars, Carbon, Cold-Finished, Standard Quality.” The ultimate tensile strength of studs and the modulus of elasticity are 635 MPa and 205 GPa (92.1 and 29,732.7 ksi), respectively. The geometry of a shear stud is shown in Fig. 3.

Preparation of specimens and testing

The geometry of the pushout specimen is shown in Fig. 4. Two substrate slabs, with a dimension of 305 x 305 x 152 mm

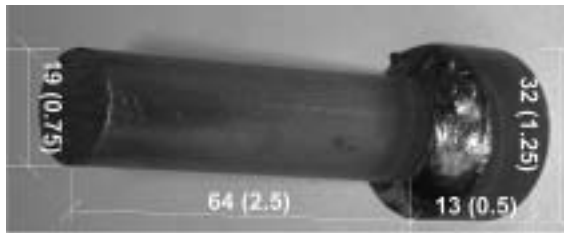


Fig. 3—Geometry of shear stud (units in mm [in.]).

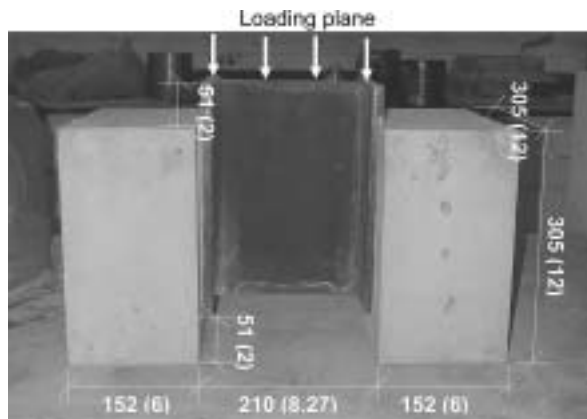


Fig. 4—Geometry of pushout specimen (units in mm [in.]) (note: stud is located in midheight of slabs and both spacing and edge distances are 101.6 mm [4 in.]).

(12 x 12 x 6 in.), were connected with a wide flange steel beam W8X40 with two shear studs welded on each side of the beam. The geometry is adopted from Ollgaard et al. (1971). During casting, the material was placed from the top of the specimen. Therefore, the steel beam remained vertical to ensure that the horizontal loading plane is parallel to the bottom of the specimen. Even though this casting orientation is different from field conditions, the pouring direction is thought to be unimportant because polyvinyl alcohol (PVA) fibers in ECC are likely to be randomly distributed in a three-dimensional state. To ensure the symmetry of the two slabs, the plywood molds were constructed using two integral side plates and a single bottom plate.

The ECC specimens were cured in air, and other specimens cured in water for 28 days. In total, 14 specimens were tested, including two specimens for each material except ECC 1 and Concrete 2, where three specimens were tested. Testing was conducted on a 2224 kN (500 kip) capacity Instron testing machine, as shown in Fig. 5. Four linear variable displacement transducers (LVDTs) were mounted on the steel beam at the level of the shear studs to measure the slip between the beam and concrete slabs. An average value was taken from these four measurements. The loading surface was ground for uniform load distribution before testing, and a ball support was used to maintain the alignment of the specimens.

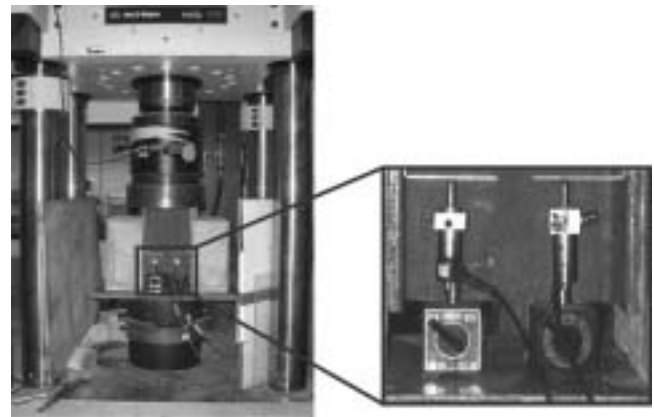


Fig. 5—Setup of pushout tests and close-up view of LVDTs.

Table 2—Material properties and structural behavior of ECC and other concrete material pushout specimens

Material	ϵ_u , %	f'_c , MPa (ksi)	E_c , GPa (10^3 ksi)	Q_n , kN (kips)	Q_m , kN (kips)	S_c , mm (in.)	w_c , μ m (in.)
Concrete 1	0.01*	52.3 ± 3.6 (7.6 ± 0.5)	28.6 ± 1.8 (4.1 ± 0.3)	174.3 ± 11.5 (39.2 ± 2.6)	125.5 ± 5.4 (28.2 ± 1.2)	2.0 ± 0.2 (0.079 ± 0.008)	~2000 (0.079)
RC 1	0.01*	53.2 ± 2.9 (7.7 ± 0.4)	28.6 ± 1.8 (4.1 ± 0.3)	175.8 ± 10.4 (39.5 ± 2.3)	149.5 ± 3.3 (33.6 ± 0.7)	3.7 ± 1.3 (0.146 ± 0.051)	~2000 (0.079)
SFRC 1	0.1*	58.7 ± 2.5 (8.5 ± 0.4)	25.4 ± 0.5 (3.7 ± 0.1)	174.0 ± 5.4 (39.1 ± 1.2)	179.7 ± 0.3 (40.4 ± 0.1)	3.9 ± 0.6 (0.154 ± 0.024)	~2000 (0.079)
ECC 1	2.5 ± 0.3	60.0 ± 2.1 (8.7 ± 0.3)	18.1 ± 1.4 (2.6 ± 0.2)	148.5 ± 8.3 (33.4 ± 1.9)	192.3 ± 11.7 (43.2 ± 2.6)	6.4 ± 1.3 (0.252 ± 0.051)	42 ± 20 (0.0017 ± 0.0008)
Concrete 2	0.01*	38.0 ± 1.4 (5.5 ± 0.2)	25.5 ± 1.2 (3.7 ± 0.2)	140.3 ± 5.8 (31.5 ± 1.3)	129.6 ± 1.9 (29.1 ± 0.4)	1.7 ± 0.1 (0.067 ± 0.004)	~2000 (0.079)
ECC 2	2.5 ± 0.4	46.0 ± 0.4 (6.7 ± 0.1)	19.3 ± 1.6 (2.8 ± 0.2)	134.3 ± 6.0 (30.2 ± 1.3)	160.9 ± 17.7 (36.2 ± 4.0)	5.8 ± 0.3 (0.228 ± 0.012)	37 ± 21 (0.0015 ± 0.0008)

Notes: ϵ_u = uniaxial tensile strain capacity; f'_c = compressive strength; E_c = modulus of elasticity; Q_n = computed strength per stud; Q_m = measured strength per stud; S_c = slip capacity (average slip at peak load); and w_c = crack width at peak load.

*Assumed value.

EXPERIMENTAL RESULTS AND DISCUSSION

Pushout behavior

Concrete and ECC—Overall, the pushout behavior of ECC specimens is significantly better than concrete ones in terms of failure mode, load capacity, slip capacity, and structural integrity. As shown in Fig. 6 and 7, the failure mode of the stud connection switched from brittle concrete fracture in concrete specimens to ductile multiple cracking of ECC and steel yielding in ECC specimens. This leads to a higher ductility of ECC/stud connections at higher peak load, as indicated in Fig. 8(a) and (b), and Fig. 9(a) and (b).

In concrete pushout tests, as loading approached the peak value (around 95% of peak value for both Concrete 1 and 2), large cracks (crack width approximately 2 mm [0.079 in.]) formed in the concrete near the shear studs and developed rapidly throughout the entire specimen as the peak load was reached. As revealed in Fig. 6, concrete specimens fractured into several pieces after testing, with fracture clearly initiated from near the head of the shear studs. The sudden drop after peak load in Fig. 8(a) and 9(a) demonstrates that after the concrete was fractured, the bearing resistance of concrete near the stud head was drastically reduced. The concrete under the shear stud was crushed due to the large bearing stress of the stud shank. The high stress concentration induced by the stiff steel stud combined with the brittle nature of concrete led to the rapid development of macro-

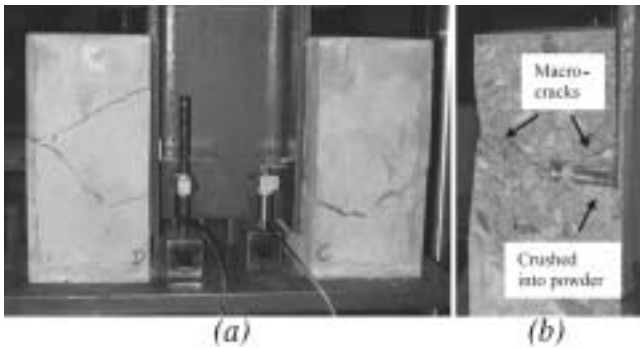


Fig. 6—Concrete pushout specimen after test showing brittle fracture failure (similar for Concrete 1 and 2). Macrocracks (crack width approximately 2 mm [0.079 in.]) are observed on: (a) outside; and (b) inside (natural fracture surface along shear stud) of specimen.

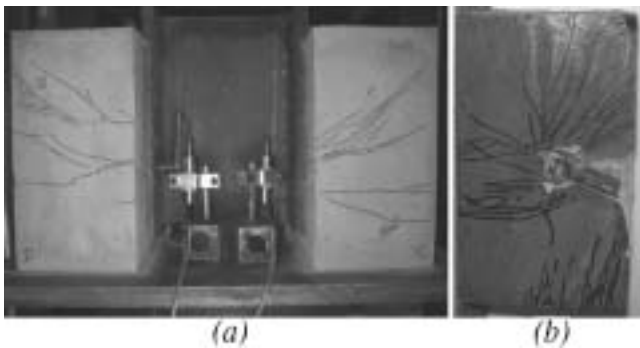


Fig. 7—ECC specimen after test showing ductile failure mode (similar for both ECC 1 and ECC 2) (crack width is approximately 40 μm [0.0016 in.], magnified by ink pen for clarity). Microcracks observed on: (a) outside; and (b) inside (cut section along shear stud) of specimen.

cracks, resulting in the catastrophic failure of concrete pushout specimens. Limited yield of the steel stud at the base of the shank was observed. However, failure of the stud was never observed.

Conversely, ECC specimens showed a ductile failure mode due to their unique strain-hardening behavior. The pushout behavior of both ECC mixtures is similar. During the linear elastic stage in Fig. 8(b) and 9(b), no cracks could be observed from the surfaces of the ECC pushout specimens (one of the test curves in Fig. 8(b) shows somewhat different behavior in the initial loading stage, possibly due to a load misalignment problem). As the load increased, a few

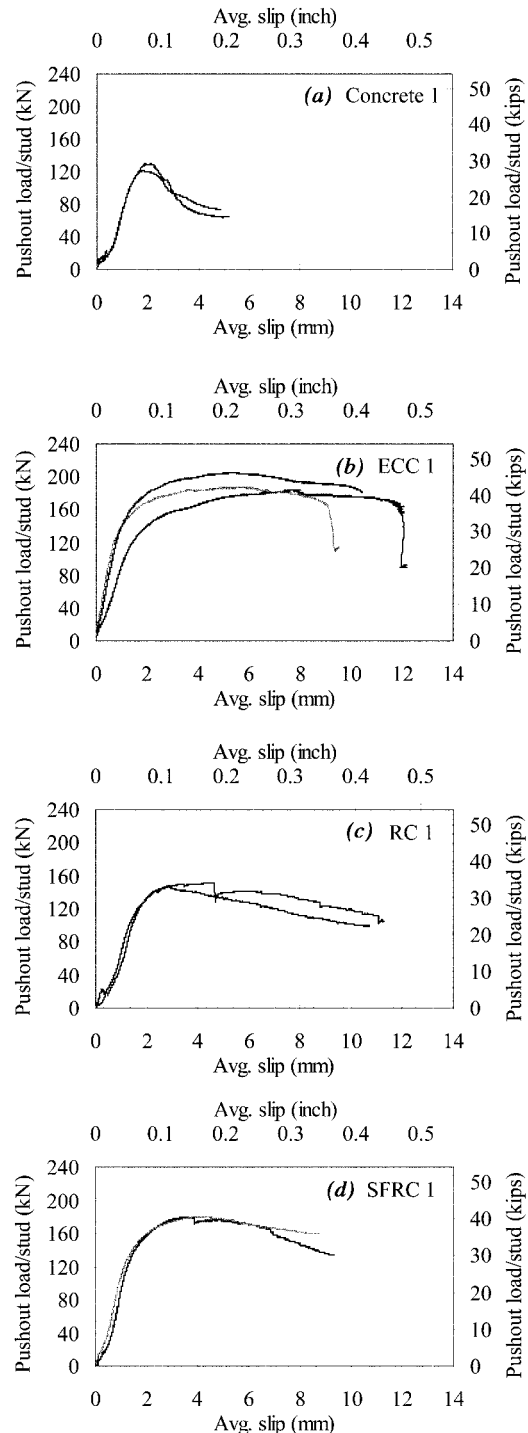


Fig. 8—Comparison of pushout load-displacement relation for Test Group 1.

microcracks appeared on the surface, accompanied by the beginning of inelastic range in the load-slip curve. When peak load was reached, more microcracks radiated from the shear stud and developed outward, as shown in Fig. 7. In some cases, a dominant crack was initiated, but diffused into many microcracks (microcrack width = $42 \pm 20 \mu\text{m}$ [$0.0017 \pm 0.0008 \text{ in.}$]) due to the ductile nature of ECC in tension and propagated slowly. Because the ECC near the stud head developed a large microcrack zone and the bearing side resisted the compressive force well, the ECC load-slip curve showed a large inelastic range (Fig. 8(b) and 9(b)). The large slip capacity revealed in the ECC specimens indicates the feasibility of engaging adjacent shear studs in sharing the shear load and improving the composite action between steel girder and concrete bridge deck.

For both ECC 1 and 2 specimens, the peak load is generally associated with the localization of one of the microcracks into a fracture, even though fracture of the steel shank

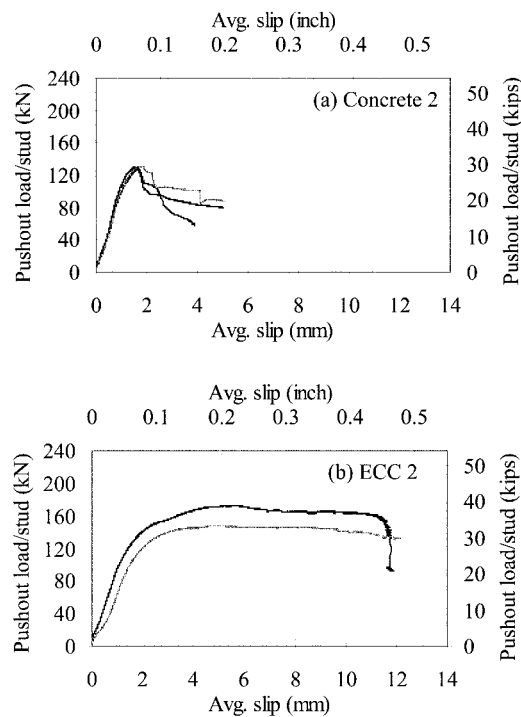


Fig. 9—Comparison of pushout load-displacement relation for Test Group 2.

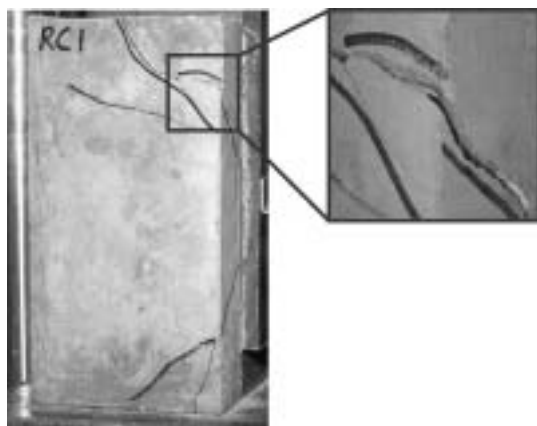


Fig. 10—RC pushout specimen after test showing crack width approximately 2 mm (0.079 in.).

eventually led to a drastic load-drop, which suggests that the ductility of the ECC and the steel stud are fully used. Overall, this indicates that the replacement of concrete by ECC materials allows for plastic yielding of the matrix material, resulting in a large deformation of the stud shank, and finally a shift of the failure from concrete brittle fracture to ductile damage process of ECC materials and eventual fracture of the stud shank after extensive plastic deformation.

As mentioned previously, a ball support was used to maintain the alignment of the specimens. Due to the relatively large friction for the ball support to rotate, however, it may be advisable to preload the specimen to mitigate alignment problems, otherwise initial loading stage may show unrealistic load-displacement response, as shown in Fig. 8(a) and (c).

Influence of reinforcement—In addition to plain concrete and ECC pushout specimens, the RC and SFRC pushout tests were conducted to consider the influence of reinforcement on pushout behavior. As expected, the addition of reinforcing bar and steel fiber in concrete pushout specimens did improve the overall structural performance to some extent, as shown in Fig. 10 and 11. Both of them, however, are inferior to ECC specimens in terms of load capacity, ductility, and structural integrity, as revealed in Fig. 7, 8, 10, and 11.

Reinforced concrete specimens developed macrocracks in the concrete rapidly near peak load with the fracture plane cutting through the thickness of the specimen. Nevertheless, the confinement of reinforcing bar led to less catastrophic softening behavior after the peak load compared with plain concrete specimens and the crack width maintained approximately 2 mm (0.079 in.). As for the SFRC, the failure process is very similar to that of RC specimens. Instead of reinforcing bar, steel fiber restrained opening of macrocracks, leading to a less catastrophic softening response.

Load-carrying capacity of stud connection

Concrete and ECC—According to the AASHTO LRFD code (developed based on the test results of Ollgaard et al. [1971]), the ultimate strength of a concrete/stud connection is as follows

$$Q_n = \min \left\{ \begin{array}{l} 0.5A_{sc}\sqrt{f'_c E_c} \\ A_{sc}F_u \end{array} \right. \quad (1)$$

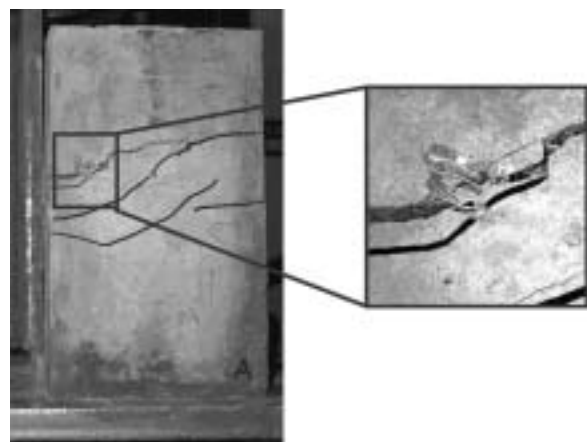


Fig. 11—SFRC pushout specimen after test showing crack width approximately 2 mm (0.079 in.).

where A_{sc} = cross-sectional area of a stud shear connector (mm^2 [in.^2]) = 285 mm^2 (0.44 in.^2) in the present experiment; f'_c = specified 28-day compressive strength of concrete (MPa [ksi]); E_c = elastic modulus of concrete (MPa [ksi]); and F_u = ultimate tensile strength of a stud shear connector (MPa [ksi]).

Table 2 shows the computed ultimate strength Q_n of a shear stud in the matrix, assuming the validity of AASHTO equation for all concrete materials, along with measured strength Q_m , slip capacity S_c , and crack width w_c . In all cases, the computed Q_n is governed by $0.5A_{sc}\sqrt{f'_c E_c}$, which is lower than $A_{sc}F_u$ (180 kN [40.5 kips]). Table 2 revealed that the measured strength of an ECC stud connection is much higher than that of a concrete stud connection even though the computed strength of the ECC stud connection should be approximately the same or even lower than that of the concrete stud connection. This suggests that material ductility of ECC plays a more significant role than does compressive strength in improving the connection response.

The measured strength of the studs in Concrete 2 is 129.6 kN (29.1 kips), within 8% of the calculated value of 140.3 kN (31.5 kips). This is as expected because the specimen setup used in this study is similar to the pushout tests performed by Ollgaard et al. (1971). In both tests, brittle fracture of concrete was the dominant factor controlling the peak load. As for Concrete 1, however, the measured strength is much lower than the computed one, which may be a result of its higher brittleness with increasing compressive strength compared with Concrete 2. Therefore, the AASHTO design equation may not give a conservative prediction when the compressive strength of concrete increases.

The measured strength Q_m of a stud in ECC 1 and ECC 2 are approximately 192.3 and 160.9 kN (43.2 and 36.2 kips), approximately 30 and 20% higher than the calculated values Q_n , and 53 and 24% higher than the measured strength of Concrete 1 and Concrete 2, respectively. This is mainly due to the fact that the compressive strength, a main contributing factor in the AASHTO equation for design of studs in concrete, is not necessarily relevant to the failure of ECC stud connections. Instead, the initial high stress concentration induced by the stud/ECC interaction caused yielding of the ECC, resulting in stress redistribution and delay of fracture localization in the ECC, thus leading to a higher load capacity of the ECC specimens. Therefore, the direct adoption of the AASHTO equation for ECC material will be excessively conservative. The actual failure mechanism of ECC specimens, that is, fracturing of the stud shank near the welds, suggests that $A_{sc}F_u$ may be used to better predict the load capacity. Furthermore, the greatly enhanced ductility and structural integrity of ECC/stud connection need to be addressed in the design procedure if ECC were to be used in stud connections of composite structures.

Influence of reinforcement—An and Cederwall (1996) indicated a 6% increase in measured strength by addition of steel reinforcing bar in plain concrete, while as revealed in Table 2, the measured strength of RC 1 increased by approximately 20% compared with that of Concrete 1. This may be attributed to the significantly higher amount of steel reinforcement in this study (approximately 0.56 and 0.86% in longitudinal and transverse directions, respectively) compared with regular design (0.3% for both directions in AASHTO LRFD empirical design). With such large reinforcement ratios, however, the measured strength of studs in RC 1 is 15% less than the computed value. This could be due to the relatively low concrete strength range tested in Ollgaard et al. (1971)

and ignoring the fracture failure mechanism in formulating the AASHTO design equation for stud connection.

Among normal concrete materials of Group 1 (Concrete 1, RC 1, and SFRC 1), SFRC 1 shows the best reinforcing result, that is, comparable measured and computed strength, even though its measured strength is still lower than that of ECC 1. It seems that the steel fibers help concrete gain higher ductility (even though still much smaller than ECC), resulting in higher structural strength than plain concrete and RC. Similarly, the extremely ductile PVA-ECC achieves the highest load capacity among all materials tested. Moreover, the slip capacity S_c (structural ductility) of the different materials increases with higher strain capacity, as shown in Table 2. Finally, it is worth mentioning that the ECC specimens show excellent structural integrity at peak load (despite the presence of many microcracks with approximately $40 \mu\text{m}$ [0.0016 in.] crack width), while the concrete and the SFRC specimens show large fractures with crack width approximately 2 mm (0.079 in.) at peak load. Hence, the repair cost for composite structures may be significantly reduced when ECC is used in stud connections.

CONCLUSIONS

This study summarizes the results of pushout tests on stud connections consisting of 14 specimens made with four different concrete materials in two groups. The main objective of this investigation was to evaluate the influence of concrete material ductility on structural response of stud connections. Four concrete materials with different tensile strain capacity (ductility) were examined. The following conclusions can be drawn from this study:

1. A new approach and material solution—exploiting ECC material ductility to overcome matrix brittle fracture failure in steel/concrete interaction zones was proposed and investigated preliminarily. The feasibility of this approach was demonstrated by a case study of shear response of stud connections, in which concrete was replaced with ECC. The test results confirm switching of the failure mode from brittle matrix fracture to ductile matrix/steel yielding and much improved structural integrity;

2. ECC specimens achieved much higher load capacity and slip capacity compared with concrete specimens with similar compressive strength due to their high tensile strain capacity. Twenty-four to fifty-three percent increases in load capacity and 220% increase in slip capacity were achieved in the test range. While concrete pushout specimens failed by brittle fracture associated with a lower ultimate strength, the ECC pushout specimens were gradually damaged by ductile yielding of ECC materials and plastic deformation of steel stud, resulting in a higher load-carrying capacity, even though fracture of the steel shank eventually led to a drastic load-drop. This phenomenon is due to the ductile nature of the ECC material that ensures a shift of failure mode from brittle concrete fracture to ductile yielding of ECC materials and eventual fracture of the stud shank after extensive plastic deformation. This significant enhancement of ductility suggests that the use of ECC material can be effective in redistributing loads among the shear studs and in improving composite action between steel girder and concrete bridge deck;

3. Material strength cannot be directly correlated to structural strength, which seems to increase with higher concrete material ductility in the present test series. Hence, good structural performance requires a balanced material

strength and ductility. ECC is one unique type of high-performance fiber-reinforced cementitious composite satisfying this requirement; and

4. The AASHTO equation for the ultimate strength of a concrete/stud connection (Eq. (1)) accurately predicts the load capacity of stud connections for normal concrete and overestimates that of higher strength concrete, possibly caused by its increased brittleness. Conversely, this equation much underestimates the load capacity of ECC/stud connections because the equation cannot take into account the actual failure mechanism of the ECC pushout specimens. A revised predictive equation governing strength of stud connections accounting for material ductility needs to be developed.

ACKNOWLEDGMENTS

This work has been supported by a research grant from the Michigan Department of Transportation to the University of Michigan with project managers D. Juntunen (2001) and R. Till (2002-2003). This support is gratefully acknowledged. G. Fischer, Y. Y. Kim, M. Lepech, S. Wang, and M. Weimann contributed to this project.

REFERENCES

AASHTO, 1998, "LRFD Bridge Design Specifications," 2nd Edition, American Association of State Highway and Transportation Officials, Washington, D.C., 1052 pp.

An, L., and Cederwall, K., 1996, "Push-Out Tests on Studs in High Strength and Normal Strength Concrete," *Journal of Construction Steel Research*, V. 36, No. 1, pp. 15-29.

Bursi, O. S., and Gramola, G., 1999, "Behavior of Headed Stud Shear Connectors under Low-Cycle High Amplitude Displacements," *Materials and Structures*, V. 32, pp. 290-297.

Driscoll, G. C., and Slutter, R. G., 1961, "Research on Composite Design at Lehigh University," *Proceedings*, National Engineering Conference, AISC, pp. 18-24.

Kanda, T.; Watanabe, W.; and Li, V. C., 1998, "Application of Pseudo Strain Hardening Cementitious Composites to Shear Resistant Structural Elements," *Fracture Mechanics of Concrete Structures*, Proceedings of FRAMCOS-3, AEDIFICATIO Publishers, Freiburg, Germany, pp. 1477-1490.

Kesner, K. E., and Billington, S. L., 2002, "Experimental Response of Precast Infill Panels made with DFRCC," *Proceedings of JCI Workshop on DFRCC*, pp. 289-298.

Li, V. C., 1993, "From Micromechanics to Structural Engineering—the Design of Cementitious Composites for Civil Engineering Applications," *Journal of Structural Engineering and Earthquake Engineering*, V. 10, No. 2, pp. 37-48.

Li, V. C., 1998, "Engineered Cementitious Composites for Structural Applications," *Materials in Civil Engineering*, pp. 66-69.

Li, V. C., 2002, "Advances in ECC Research," *Concrete: Material Science to Application—A Tribute to Surendra P. Shah*, SP-206, P. Balaguru, A. Naaman, and W. Weiss, eds., American Concrete Institute, Farmington Hills, Mich., pp. 373-400.

Oehlers, D. J., and Foley, L., 1985, "The Fatigue Strength of Stud Shear Connections in Composite Beams," *Proceedings of the Institute of Civil Engineering*, London, England, Part 2, 79, pp. 349-364.

Ollgaard, J. G.; Slutter, R. G.; and Fisher, J. W., 1971, "Shear Strength of Stud Connectors in Lightweight and Normal-Weight Concrete," *AISC Engineering Journal*, pp. 55-64.

Parra-Montesinos, G., and Wight, J. K., 2000, "Seismic Response of Exterior RC Column-to-Steel Beam Connections," *Journal of Structural Engineering*, pp. 1113-1121.

Viest, I. M., 1956a, "Test of Stud Shear Connectors, Parts I, II, III and IV," Engineering, Test Data, Nelson Stud Welding, Lorain, Ohio, 32 pp.

Viest, I. M., 1956b, "Investigation of Stud Shear Connectors for Composite Concrete and Steel T-Beams," *ACI JOURNAL, Proceedings* V. 53, No. 8, pp. 875-891.

Viest, I. M., 1960, "Review of Research on Composite Steel-Concrete Beams," *Journal of the Structural Division*, ASCE, V. 86, No. ST6, pp. 1-21.

Yen, J. R.; Lin, Y.; and Lai, M. T., 1997, "Composite Beams Subjected to Static and Fatigue Loads," *Journal of Structural Engineering*, pp. 765-771.